Biochimica et Biophysica Acta 1788 (2009) 1193–1203

Contents lists available at ScienceDirect

Biochimica et Biophysica Acta

journal homepage: www.elsevier.com/locate/bbamem

Cell specificity, anti-inflammatory activity, and plausible bactericidal mechanism of designed Trp-rich model antimicrobial peptides

Ka Hyon Park [a,1], Yong Hai Nan [a,1], Yoonkyung Park [a,b], Jae Il Kim [c], Il-Seon Park [a,d], Kyung-Soo Hahm [a,d], Song Yub Shin [a,d,*]

[a] Department of Bio-Materials, Graduate School and Research Center for Proteineous Materials, Chosun University, Gwangju 501-759, Korea
[b] Department of Biotechnology, Chosun University, Gwangju 501-759, Korea
[c] Department of Life Science, Gwangju Institute of Science and Technology, Gwangju 500-712, Korea
[d] Department of Cellular and Molecular Medicine, School of Medicine, Chosun University, Gwangju 501-759, Korea

ARTICLE INFO

Article history:
Received 13 November 2008
Received in revised form 29 January 2009
Accepted 27 February 2009
Available online 11 March 2009

Keywords:
Anti-inflammatory activity
Bactericidal mechanism
Cell specificity
Trp-rich model antimicrobial peptide

ABSTRACT

To develop novel short Trp-rich antimicrobial peptides (AMPs) with potent cell specificity (targeting bacteria but not eukaryotic cells) and anti-inflammatory activity, a series of 11-meric Trp-rich model peptides with different ratios of Leu and Lys/Arg residues, XXWXXWXXWXX-NH_2 (X indicates Leu or Lys/Arg), was synthesized. $K_6L_2W_3$ displayed an approximately 40-fold increase in cell specificity, compared with the natural Trp-rich AMP indolicidin (IN). Lys-containing peptides (K_8W_3, K_7LW_3 and $K_6L_2W_3$) showed approximately 2- to 4-fold higher cell specificities than did their counterparts, the Arg-containing peptides (R_8W_3, R_7LW_3 and $R_6L_2W_3$), indicating that multiple Lys residues are more important than multiple Arg residues in the design of AMPs with good cell specificity. The excellent resistance of D-enantiomers ($K_6L_2W_3$-D and $R_6L_2W_3$-D) and Orn/Nle-containing peptides ($O_6L_2W_3$ and $O_6L_2W_3$) to trypsin digestion compared with the rapid breakdown of the L-enantiomers ($K_6L_2W_3$ and $R_6L_2W_3$), highlights the clinical potential of such peptides. $K_6L_2W_3$, $R_6L_2W_3$, $K_6L_2W_3$-D and $R_6L_2W_3$-D caused weak dye leakage from bacterial membrane-mimicking negatively charged EYPG/EYPE (7:3, v/v) liposomes. Confocal microscopy showed that these peptides penetrated the cell membrane of *Escherichia coli* and accumulated in the cytoplasm, as observed for buforin-2. Gel retardation studies revealed that the peptides bound more strongly to DNA than did IN. These results suggested that one possible peptide bactericidal mechanism may relate to the inhibition of intracellular functions via interference with DNA/RNA synthesis. Furthermore, some model peptides, containing $K_6L_2W_3$, $K_5L_3W_3$, $R_6L_2W_3$, $O_6L_2W_3$, $O_6L_2W_3$, and $K_6L_2W_3$-D inhibited LPS-induced inducible nitric oxide synthase (iNOS) mRNA expression, the release of nitric oxide (NO) following LPS stimulation in RAW264.7 cells and had powerful LPS binding activities at bactericidal concentrations. Collectively, our results indicated that these peptides have potential for future development as novel antimicrobial and anti-inflammatory agents.

1. Introduction

A rapid increase in the emergence of bacteria resistant to conventionally used antibiotics has occurred in recent years. The increasing prevalence of multidrug-resistant bacteria necessitates the development of new antibiotics to combat infections by these bacteria [1–4]. Antimicrobial peptides (AMPs), isolated from a wide range of animal, plant, and bacterial species, are ubiquitous in nature and are thought to be important in innate immunity and host defenses against infectious agents [1–4]. Because of their rapid killing action, highly selective toxicity, and because bacteria cannot easily develop resistance against the peptides, AMPs are considered as potential alternatives to conventional antibiotics [5,6]. Most AMPs do not target specific molecular receptors of pathogens but rather interact with and permeabilize microbial membranes [7,8].

A comparison of AMP sequences reveals that two types of side chains are essential for antimicrobial activity. Cationic side chains, such as those of Arg and Lys, are thought to mediate peptide interactions with negatively charged membranes and/or cell walls of Gram-negative bacteria [9–12]. Bulky hydrophobic side chains, such as those of Ile, Leu, Phe, or Trp, occur frequently in AMPs, presumably providing lipophilic anchors that ultimately induce membrane disruption [9–12]. It has been reported that the

* Corresponding author. Department of Cellular and Molecular Medicine, School of Medicine, Chosun University, Gwangju 501-759, Korea. Tel.: +82 62 230 6769; fax: +82 62 227 8345.
E-mail address: syshin@chosun.ac.kr (S.Y. Shin).
[1] These authors contributed equally to this work.

0005-2736/$ – see front matter © 2009 Elsevier B.V. All rights reserved.
doi:10.1016/j.bbamem.2009.02.020

antimicrobial activity of AMPs is governed by the positive charge and hydrophobicity of residues, and there should be a proper balance between cationic and hydrophobic residues to avoid toxicity toward mammalian cells [9–12].

In recent years, there has been an increasing interest in understanding the mechanisms of action of short Trp-rich peptides [13–16]. Trp has a strong ability to insert into membranes and Trp-rich peptides partition into membranes [13,14]. A well-studied example of a Trp-rich peptide is the 13-meric indolicidin (IN) isolated from the cytoplasmic granules of bovine neutrophils [17]. Although IN displays activity against a wide range of targets, including Gram-positive and Gram-negative bacteria, fungi, and protozoa, the relatively high toxicity of IN toward mammalian cells prevents its use as an antibiotic. Therefore, much effort has been directed to decreasing toxicity for mammalian cells and to improving IN antimicrobial activity [18–21].

In this study, we designed novel Trp-rich model AMPs with high antimicrobial activities, coupled with no or less hemolytic activities (*i.e.* with higher cell specificity/therapeutic index), and that were shorter in length than the natural Trp-rich AMP IN. A series of 11-mer cationic Trp-rich model peptides, with different ratios of Lys and Leu residues, and with the structure XXWXXWXXWXX-NH_2 (X represents Leu or Lys), was synthesized. All these peptides (K_8W_3, K_7LW_3, K_7LW_3, $K_6L_2W_3$, $K_5L_3W_3$, $K_4L_4W_3$, $K_3L_5W_3$ and $K_2L_6W_3$) have net positive charges, ranging between +3 and +9, and have different hydrophobicities. To investigate the functional difference between Lys and Arg in the cell specificity of cationic Trp-rich model peptides, Lys→Arg substitution analogs (R_8W_3, R_7LW_3 and $R_6L_2W_3$) were also prepared. In addition, to increase the stability of the peptides to endogenous proteases, D-enantiomers ($K_6L_2W_3$-D and $R_6L_2W_3$-D) with D-amino acids, and two analogs ($O_6L_2W_3$ and $O_6X_2W_3$) containing Orn and/or Nle, were constructed. Antimicrobial activities against Gram-positive and Gram-negative bacterial strains including antibiotic-resistant clinical isolates, and the ability of peptides to cause hemolysis, were examined. Tryptophan fluorescence spectroscopy was used to explore the specificities of peptides for liposomes that mimicked bacterial or eukaryotic cells. Furthermore, the mechanisms by which the peptides killed bacteria were investigated by measuring peptide ability to cause leakage of a fluorescent dye from bacterial membranes-mimicking lipid vesicles. In addition, to determine peptide localization, confocal microscopy was performed after treatment of a wild-type *Escherichia coli* strain with FITC-labeled peptides.

Lipopolysaccharide (LPS; endotoxin) is the major outer surface membrane component of almost all Gram-negative bacteria and acts as an extremely strong stimulator of mononuclear phagocytes (monocytes and macrophages), which are part of the innate immune system of diverse eukaryotic species ranging from insects to humans [22,23]. The activation mechanism of macrophages by LPS starts when LPS binds with LPS-binding protein (LBP), accelerating the binding of CD14, the primary receptor of LPS, which is expressed mainly on macrophages [24]. The LPS-LBP-CD14 complex initiates intracellular signaling by interacting with the transmembrane protein Toll-like receptor-4 (TLR-4), which activates the NF-κB transcription factor, resulting in the production and secretion of inflammatory cytokines, including tumor necrosis factor-α (TNF-α), interleukin-6 (IL-6), nitric oxide (NO) and others [24–26].

Recent studies have demonstrated that in addition to their antimicrobial activities, a few cathelicidin-derived AMPs, such as LL-37, IN, bactenecin, BMAP-27, and β-defensin, have the potential to inhibit LPS-induced cellular cytokine and/or nitric oxide (NO) release by binding directly to LPS or by blocking the binding of LPS to LPS-binding protein (LBP) [24–31]. These properties make these AMPs attractive drug candidates for treatment of endotoxin shock and sepsis caused by Gram-negative bacterial infections [24–31].

Therefore, to investigate whether our designed antimicrobial peptides show anti-inflammatory activities when tested with immune cells, peptide inhibition of NO production and iNOS mRNA expression in LPS-stimulated mouse macrophage RAW264.7 cells were examined. LPS binding activities of IN and analogs were explored by the chromogenic *Limulus* amebocyte lysate (LAL) assay. These results will help in the design of novel short antimicrobial peptides with potent antimicrobial and anti-inflammatory activities.

2. Materials and methods

2.1. Materials

Rink amide 4-methylbenzhydrylamine (MBHA) resin, fluoren-9-yl-methoxycarbonyl (Fmoc)-amino acids and other reagents for the peptide synthesis were purchased from Calbiochem-Novabiochem (La Jolla, CA). Egg yolk L-phosphatidylcholine (EYPC), egg yolk L-phosphatidylethanolamine (EYPE), egg yolk L-phosphatidyl-DL-glycerol (EYPG), LPS (lipopolysaccharide from *E. coli* O111:B4), calcein, gramicidin D (GD), trypsin (from bovine pancreas, EC 3.4.21.4) and polymyxin B were supplied by Sigma Chemical Co (St. Louis, MO). DMEM and fetal bovine serum (FBS) were supplied by HyClone (SeouLin, Bioscience, Korea). RAW 264.7 cells were purchased from American Type Culture Collection (Bethesda, MD). All other reagents were of analytical grade. The buffers were prepared in double glass-distilled water.

2.2. Peptide synthesis

Peptides listed in Table 1 were prepared using the standard Fmoc-based solid-phase synthesis technique on Rink amide MBHA resin support. DCC (dicyclohexylcarbodiimide) and HOBt (N-hydroxybenzotriazole) were used as coupling reagents, and ten-fold excess Fmoc-amino acids added during every coupling cycle. After cleavage and deprotection with a mixture of trifluoroacetic acid/water/thioanisole/phenol/ethanedithiol/triisopropylsilane (81.5:5:5:5:2.5:1, v/v) for 2 h at room temperature, crude peptides were repeatedly extracted with diethyl ether and purified by reverse-phase HPLC on a preparative Vydac C_{18} column (15 μm, 20×250 mm) using an appropriate 0–90% water/acetonitrile gradient in the presence of 0.05% trifluoroacetic acid. The final purity of the peptides (>98%) was assessed by reverse-phase HPLC on an analytical Vydac C_{18} column (4.6×250 mm, 300 Å, 5-μm particle size). The molecular masses of purified peptides were determined using MALDI-TOF MS (matrix-assisted laser-desorption ionization-time-of-flight mass spectrometry) (Shimadzu, Japan). Peptide concentrations were determined by amino acid analysis (Hitachi Model, 8500 A, Japan) and relative hydrophobicity measured from the retention times on a C_{18} reverse-phase analytical column.

2.3. Antimicrobial activity (MIC)

The antibacterial activities of peptides against three Gram-positive bacterial strains and three Gram-negative bacterial strains were examined in sterile 96-well plates with the broth microdilution method. Aliquots (100 μl) of a bacterial suspension at 2×10^6 colony-forming units (CFU)/ml in 1% peptone were added to 100 μl of peptide solution (serial 2-fold dilutions in 1% peptone). After incubation for 18–20 h at 37 °C, bacterial growth inhibition was determined by measuring absorbance at 600 nm with a Microplate autoreader EL 800 (Bio-Tek Instruments). The minimal inhibitory concentration (MIC) is defined as the minimum peptide concentration that inhibits bacteria growth. Three types of Gram-positive bacteria (*Bacillus subtilis* [KCTC 3068], *Staphylococcus epidermidis* [KCTC 1917] and *Staphylococcus aureus* [KCTC 1621]) and three types of Gram-negative bacteria (*Escherichia coli* [KCTC 1682], *Pseudomonas aeruginosa* [KCTC 1637] and *Salmonella typhimurium* [KCTC 1926]) were procured from the Korean Collection for Type Cultures (KCTC) at the Korea Research

Table 1
Amino acid sequences, calculated and observed molecular masses, net charges, and RP-HPLC retention times of the Trp-rich model peptides designed and synthesized in this study.

Peptides	Amino acid sequences	Molecular MS		Net charge	Retention times (RT)[b]
		Calculated	Measured[a]		
K_8W_3	KKWKKWKKWKK-NH_2	1601.1	1601.0	+9	16.00
K_7LW_3	KLWKKWKKWKK-NH_2	1586.0	1585.7	+8	17.85
$K_6L_2W_3$	KLWKKWKKWLK-NH_2	1571.0	1570.4	+7	20.92
$K_5L_3W_3$	KLWKLWKKWLK-NH_2	1556.0	1555.3	+6	24.03
$K_4L_4W_3$	KLWKLWLKWLK-NH_2	1540.9	1541.7	+5	27.61
$K_3L_5W_3$	KLWKLWLKWLL-NH_2	1525.9	1525.7	+4	31.87
$K_2L_6W_3$	KLWLLWLKWLL-NH_2	1510.9	1511.8	+3	36.44
R_8W_3	RRWRRWRRWRR-NH_2	1825.1	1825.7	+9	19.55
R_7LW_3	RLWRRWRRWRR-NH_2	1782.1	1782.3	+8	19.30
$R_6L_2W_3$	RLWRRWRRWLR-NH_2	1739.1	1739.7	+7	21.56
$O_6L_2W_3$	OLWOOWOOWLO-NH_2	1486.9	1487.3	+7	20.54
$O_6X_2W_3$	OXWOOWOOWXO-NH_2	1486.9	1486.7	+7	20.83
$K_6L_2W_3$-D	klwkkwkkwlk-NH_2	1571.0	1571.2	+7	21.00
$R_6L_2W_3$-D	rlwrrwrrwlr-NH_2	1739.1	1738.9	+7	21.69
Indolicidin (IN)	ILPWKWPWWPWRR-NH_2	1909.3	1909.3	+4	29.63

[a] Molecular masses were determined by MALDI-TOF-MS. O and X indicate Orn (ornithine) and Nle (norleucine), respectively. Small letters represent D-type amino acids.
[b] Retention time (RT) was measured using a C_{18} reverse-phase analytical column (5 μm; 4.6×250 mm; Vydac). Peptides were eluted for 60 min, using a linear gradient of 0% to 90% (v/v) acetonitrile in water containing 0.05% (v/v) trifluoroacetic acid.

Institute of Bioscience and Biotechnology (KRIBB). Methicillin-resistant *Staphylococcus aureus* (MRSA) (CCARM 3001 and CCARM 3543) and multidrug-resistant *Pseudomonas aeruginosa* (MDRPA) (CCARM 2095 and CCARM 2109) were obtained from the Culture Collection of Antibiotic-Resistant Microbes (CCARM) at Seoul Women's University in Korea.

2.4. Hemolytic activity (MHC)

Fresh human red blood cells (hRBCs) were washed 3 times with PBS (35 mM phosphate buffer, 0.15 M NaCl, pH 7.4) by centrifugation for 7 min at 1000×*g*, and resuspended in PBS. The peptide solutions (serial 2-fold dilutions in PBS) were added to 100 ml of hRBC suspension [4% (v/v) in final] in PBS to a final volume of 200 μl, and incubated for 1 h at 37 °C. Samples were centrifuged at 1000×*g* for 5 min, and hemoglobin release monitored by measuring supernatant absorbance at 405 nm with Microplate ELISA Reader. MHC is defined as the minimal peptide concentration that producing 5% hemolysis. As negative and positive controls, hRBCs in PBS (A_{blank}) and 0.1% Triton X-100 (A_{triton}) were employed, respectively. The hemolysis percentage was calculated according to the equation:

$$\%\ \text{hemolysis} = 100 \times \left[\left(A_{\text{sample}} - A_{\text{blank}}\right) / \left(A_{\text{triton}} - A_{\text{blank}}\right)\right]$$

2.5. Resistance to proteolytic digestion

Bacteria (*E. coli* and *S. aureus*) were grown overnight for 18 h at 37 °C in 10 ml of LB broth and then 10 μl of this culture was inoculated into 10 ml of fresh LB and incubated for an additional 3 h at 37 °C to obtain mid-logarithmic phase organisms. For the radial diffusion assay method, a bacteria suspension (2×10^6 CFU/ml in LB) was mixed with 0.7% agarose. The mixture was poured into a 10-cm petri dish after rapidly dispersing. Five microliters of an aqueous peptide stock solution (10 mg/mL) were added to 25 μl of 0.2 μg/ml trypsin solution in PBS, receptively, and incubated at 37 °C for 6 h. The reaction was stopped by freezing with liquid nitrogen, and then ten-microliters aliquots were placed in each circle paper (≈6 mm in diameter) put on the agarose plates and then incubated at 37 °C for overnight. The diameters of the bacterial clearance zones surrounding the circle paper were measured for the quantitation of inhibitory activities. For the broth microdilution assay method, aliquots (100 μl) of a bacterial suspension (2×10^6 CFU/ml in 1% peptone) were added to 100 μl of each peptide in 1% peptone (final peptide concentration: 2× MIC for bacteria). After incubation for 18–20 h at 37 °C, bacterial growth inhibition was determined by measuring absorbance at 600 nm with a Microplate autoreader EL 800 (Bio-Tek Instruments).

2.6. Preparation of small unilamellar vesicles (SUVs)

Small unilamellar vesicles were prepared with a standard procedure using the required amounts of EYPE/EYPG (7:3, w/w) or EYPC/cholesterol (10:1, w/w) for tryptophan fluorescence. Dry lipids were dissolved in chloroform in a small glass vessel. Solvents were removed by rotary evaporation to form a thin film on the wall of a glass vessel and lyophilized overnight. Dried thin films were resuspended in Tris–HCl buffer by vortex mixing. Lipid dispersions were sonicated on ice water for 10–20 min with a titanium-tip ultrasonicator until the solution became transparent.

2.7. Tryptophan fluorescence blue shift

The fluorescence emission spectrum of tryptophan of peptides was monitored in aqueous Tris–HCl buffer, Tris–HCl buffer containing 1.5 M NaCl and in the presence of vesicles composed of either EYPE/EYPG (7:3 w/w) SUVs or EYPC/cholesterol (10:1 w/w) SUVs. In these fluorometric studies, small unilamellar vesicles (SUVs) were used to minimize differential light scattering effects [32,33]. Tryptophan fluorescence measurements were obtained using a model RF-5301PC spectrophotometer (Shimadzu, Japan). Each peptide was added to 3 ml of Tris–HCl buffer (10 mM Tris, 0.1 mM EDTA, 150 mM NaCl, pH 7.4) containing 0.6 mM liposomes (pH 7.4), and the peptide/liposome mixture (molar ratio of 1:200) allowed to interact at 20 °C for 10 min. The fluorescence was excited at 280 nm, and emission scanned from 300 to 400 nm.

2.8. Dye leakage

Calcein-entrapped LUVs composed of EYPE/EYPG (7:3, w/w) were prepared by vortexing the dried lipid in dye buffer solution (70 mM calcein, 10 mM Tris, 150 mM NaCl, 0.1 mM EDTA, pH 7.4). The suspension was subjected to 10 frozen-thaw cycles in liquid nitrogen and extruded 21 times through polycarbonate filters (two stacked 100-nm pore size filters) with a LiposoFast extruder (Avestin, Inc., Canada). Untrapped calcein was removed by gel filtration on a Sephadex G-50 column. The concentration of calcein-entrapped LUVs was determined in triplicate by phosphorus

Table 2
Minimal inhibitory concentrations (MICs) of the peptides against Gram-negative and Gram-positive bacterial strains.

Peptide	MIC[a] (μM)					
	Gram-negative bacteria			Gram-positive bacteria		
	E. coli [KCTC 1682]	*P. aeruginosa* [KCTC 1637]	*S. typhimurium* [KCTC 1926]	*B. subtilis* [KCTC 3068]	*S. epidermidis [KCTC 1917]*	*S. aureus* [KCTC 1621]
K_8W_3	4	2	1	2	2	4
K_7LW_3	2	2	1	2	2	4
$K_6L_2W_3$	2	2	1	2	2	2
$K_5L_3W_3$	2	2	1	4	2	2
$K_4L_4W_3$	4	4	2	4	4	2
$K_3L_5W_3$	8	8	4	8	8	4
$K_2L_6W_3$	32	16	32	32	32	32
R_8W_3	8	8	4	4	2	8
R_7LW_3	8	8	4	4	2	4
$R_6L_2W_3$	8	8	2	4	2	4
$O_6L_2W_3$	2	4	2	4	2	4
$O_6X_2W_3$	2	4	2	2	2	4
$K_6L_2W_3$-D	4	4	2	4	4	4
$R_6L_2W_3$-D	4	4	2	2	4	2
Indolicidin (IN)	4	8	4	2	8	4

analysis [34]. Calcein leakage from LUVs was monitored by measuring fluorescence intensity at an excitation wavelength of 490 nm and emission wavelength of 520 nm on a model RF-5301PC spectrophotometer. For determination of 100% dye-release, 20 μl 10% Triton-X100 in Tris-buffer was added to dissolve the vesicles. The percentage of dye leakage caused by the peptides was calculated as follows:

$$\%\ \text{Dye leakage} = 100 \times [(F - F_0) / (F_t - F_0)]$$

where F is the fluorescence intensity achieved at 5 min after peptide addition, and F_0 and F_t represent fluorescence intensities without the peptides and with Triton X-100, respectively.

2.9. Confocal laser-scanning microscopy

E. coli cultures were grown to the mid-logarithmic phase. *E. coli* cells (10^7 CFU/ml) in 10 mM PBS, pH 7.4 were incubated with FITC-labeled peptides (5 μg/ml) at 37 °C for 30 min. Next, cells were washed with PBS and immobilized on a glass slide. FITC-labeled peptides were observed with an Olympus IX 70 confocal laser-scanning microscope (Japan). Fluorescent images were obtained with a 488-nm band-pass filter for FITC excitation.

2.10. DNA binding assay

Gel retardation experiments were performed by mixing 100 ng of the plasmid DNA (pBluescript II SK^+) with increasing amounts of peptide in 20 μl of binding buffer (5% glycerol, 10 mM Tris–HCl, pH 8.0, 1 mM EDTA, 1 mM dithiothreitol, 20 mM KCl, and 50 μg/ml bovine serum albumin). Reaction mixtures were incubated at room temperature for 1 h. Subsequently, 4 μl of native loading buffer was added (10% Ficoll 400, 10 mM Tris–HCl, pH 7.5, 50 mM EDTA, 0.25% bromophenol blue, and 0.25% xylene cyanol), and a 20 μl aliquot subjected to 1% agarose gel electrophoresis in 0.5×Tris borate-EDTA buffer (45 mM Tris-borate and 1 mM EDTA, pH 8.0). The plasmid DNA used was purified by CsCl-gradient ultracentrifugation to select the closed circular form of the plasmid.

2.11. Cell culture

RAW 264.7 cells were purchased from the American Type Culture Collection (Manassas, VA) and cultured in DMEM supplemented with 10% fetal bovine serum and antibiotic–antimyotic solution (100 U/ml penicillin, 100 g/ml streptomycin and 25 g amphotericin B) in 5% CO_2 at 37 °C. Cultures were passed every 3 to 5 days, and cells were detached by brief trypsin treatment, and visualized with an inverted microscope.

2.12. Cytotoxicity (MTT proliferation assay)

Cytotoxicity of peptides against RAW 264.7 cells was determined using the MTT assay as reported previously [35], with minor modifications. RAW 264.7 cells were seeded on 96-well microplates at a density of 2×10^4 cells/well in 150 μl DMEM containing 10% fetal bovine serum. Plates were incubated for 24 h at 37 °C in 5% CO_2. Peptide solutions (20 μl) (serial 2-fold dilutions in DMEM) were added, and the plates further incubated for 2 days. Wells containing cells without peptides served as controls. Subsequently, 20 μl MTT solution (5 mg/ml) was added in each well, and the plates were incubated for a further 4 h at 37 °C. Precipitated MTT formazan was dissolved in 40 μl of 20% (w/v) SDS containing 0.01 M HCl for 2 h. Absorbance at 570 nm was measured using a microplate ELISA reader (Molecular Devices, Sunnyvale, CA). Cell survival was expressed as a percentage of the ratio of A_{570} of cells treated with peptide to that of cells only.

Table 3
Cell specificities (therapeutic indices) of the peptides used in this study.

Peptide	GM (μM)[a]	MHC (μM)[b]	Therapeutic Index (TI)[c] (MHC/GM)
K_8W_3	2.5	400<	320.0
K_7LW_3	2.2	400<	363.6
$K_6L_2W_3$	2.0	400<	400.0
$K_5L_3W_3$	2.2	100	45.5
$K_4L_4W_3$	3.3	6.25	1.9
$K_3L_5W_3$	6.7	3.125	0.5
$K_2L_6W_3$	29.3	1.56	0.1
R_8W_3	5.6	400<	142.8
R_7LW_3	5.0	400<	160.0
$R_6L_2W_3$	4.6	400	86.9
$O_6L_2W_3$	3.0	400<	266.6
$O_6X_2W_3$	2.6	400	153.8
$K_6L_2W_3$-D	3.6	400	111.1
$R_6L_2W_3$-D	3.0	400	133.3
Indolicidin (IN)	4.8	50	10.4

[a] The geometric mean (GM) of the MIC values of the peptides acting against all six bacterial strains shown in the table.
[b] The MHC (minimal hemolytic concentration) is the peptide concentration causing 5% hemolysis.
[c] The ratio of the MHC (μM) to the geometric mean MIC (μM). Larger values indicate greater cell specificity.

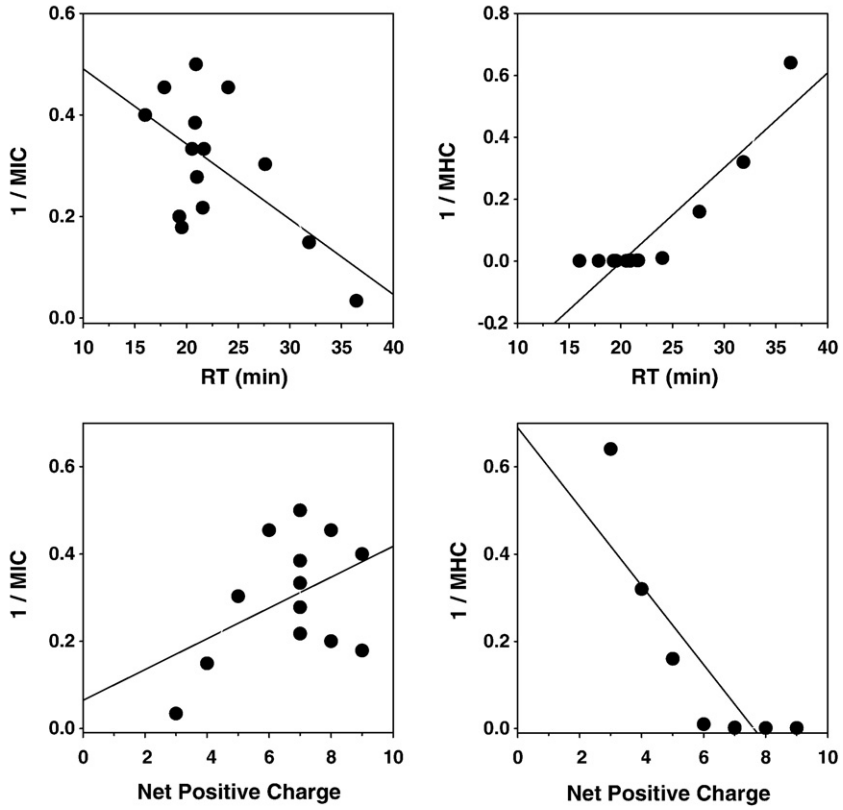

Fig. 1. Relationships of cationicity and hydrophobicity of the peptides between and antimicrobial activity and hemolytic activity. The line was fitted by the linear regression. Each point represents one peptide.

2.13. Nitric oxide (NO) production from LPS-stimulated RAW 264.7 cells

Nitrite accumulation in culture media was used as an indicator of nitric oxide (NO) production [36]. Cells were plated at a density of 5×10^5 cells ml^{-1} in 96-well culture plates, and stimulated with LPS (20 ng/ml) from *E. coli* O111:B4 (Sigma) in the presence or absence of peptides for 24 h. Isolated supernatant fractions were mixed with an equal volume of Griess reagent (1% sulfanilamide, 0.1% naphthylethylenediamine dihydrochloride, and 2% phosphoric acid) and incubated at room temperature for 10 min. Nitrite production was measured by absorbance at 540 nm, and the concentrations were determined using a standard curve generated with $NaNO_2$.

2.14. Determination of iNOS mRNA expression

RAW 264.7 cells were plated in six-well plates (5×10^5 cells/well) and cultured overnight. Cells were stimulated without (negative control) or with 20 ng/ml LPS in the presence or absence of peptide in DMEM supplemented with 10% bovine serum for 3 h. After stimulation, the cells were detached from the wells and washed once with phosphate-buffered saline (PBS). Competitive RT-PCR was performed as described previously [37]. Briefly, total RNA was extracted using TriReagent (Molecular Research Center, Cincinnati, OH) according to the manufacturer's instructions. RNA samples were used as the template in RT-PCR. The cDNA products of iNOS were amplified in the presence of 3′ (5′-CTGCAGCACTTGGATCAGGAACCTG-3′) and 5′ (5′-GGGAGTAGCCTGTGTGCACCTGGAA-3′) primers. Equal amounts of RNA were reversely transcribed into cDNA with oligo(dT) 15 primers. PCR was performed with cDNA and individual primers. For competitive RT-PCR analysis of iNOS mRNA, we used an internal standard, specifically, a cDNA fragment with the central 80 bp deleted. Samples were heated to 94 °C for 5 min, and cycled 40 times at 94 °C for 1 min, 55 °C for 1.5 min, and 94 °C for 1 min, followed by an additional extension step of 72 °C for 5 min. The PCR-amplified products were electrophoresed on an 8% polyacrylamide gel, followed by ethidium bromide staining. We obtained 311- and a 231-bp product with the RNA and internal standard, respectively.

2.15. LPS binding assay

The ability of the peptides to neutralize LPS was determined using a commercially available *Limulus* amebocyte lysate (LAL) assay (Kinetic-QCL 1000 kit; BioWhittaker, Walkersville, MD, USA) [38,39].

Table 4
Antimicrobial activities of peptides against antibiotic-resistant clinical isolates.

Peptides	MIC (μM)[a]			
	MRSA 1[b] [CCARM 3001]	MRSA 2 [CCARM 3543]	MDRPA 1[c] [CCARM 2095]	MDRPA 2 [CCARM 2109]
K_8W_3	8	4	8	8
K_7LW_3	8	4	8	8
$K_6L_2W_3$	4	2	8	8
$K_5L_3W_3$	4	4	4	8
$K_4L_4W_3$	8	4	16	16
$K_3L_5W_3$	4	4	8	16
$K_2L_6W_3$	64	32	64	> 64
R_8W_3	8	4	16	16
R_7LW_3	8	2	16	16
$R_6L_2W_3$	8	2	16	16
$O_6L_2W_3$	8	2	8	16
$O_6X_2W_3$	8	2	8	16
$K_6L_2W_3$-D	8	2	16	32
$R_6L_2W_3$-D	8	2	16	32
Indolicidin (IN)	8	8	32	32

[a] Determined in three independent experiments, each performed in triplicate.
[b] Methicillin-resistant *Staphylococcus aureus*.
[c] Multidrug-resistant *Pseudomonas aeruginosa*.

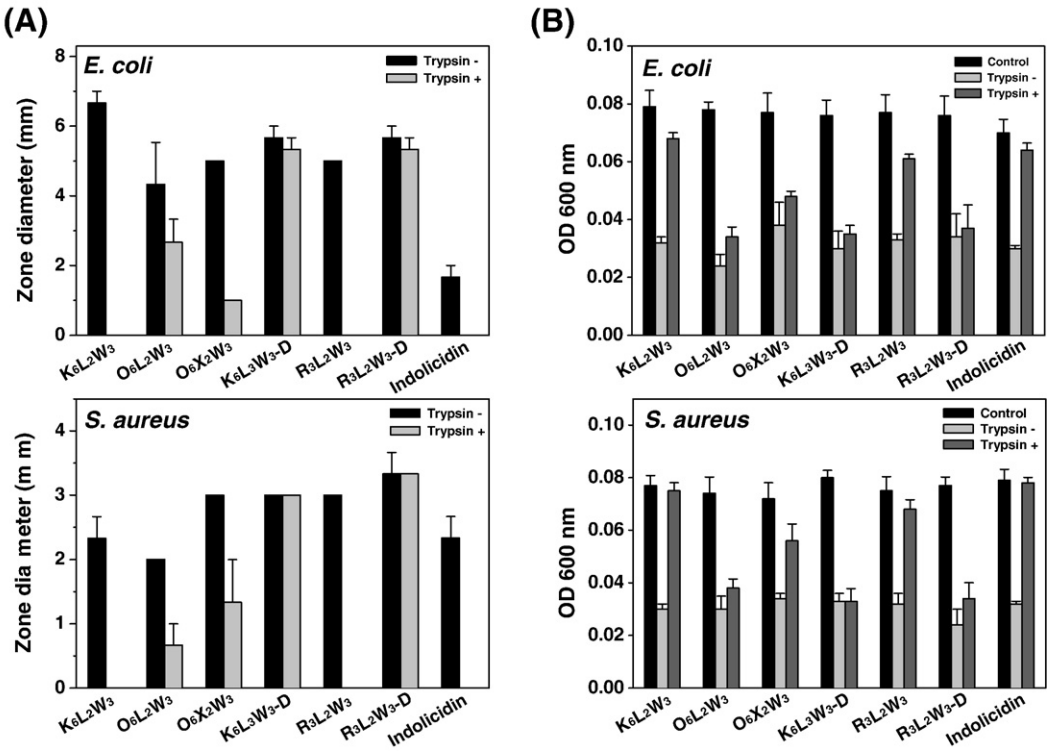

Fig. 2. Inhibition of antimicrobial activity of the peptides by trypsin assessed using the radial diffusion assay (A) and broth microdilution assay (B) methods.

Briefly, 25 μl of serially diluted peptide was added in duplicate to 25 μl of *E. coli* O55:B5 LPS containing 0.5 U/ml endotoxin for 30 min at 37 °C, followed by incubation with 50 μl of amoebocyte lysate reagent for 10 min. Absorbance at 405 nm was measured 10 and 16 min after the addition of 100 μl of the chromogenic substrate, Ac-Ile-Glu-Ala-Arg-*p*-nitroanilide. The amount of non-bound LPS was extrapolated from a standard curve, and percentage inhibition calculated as: [(amount of free LPS in control samples) − (amount of free LPS in test samples)] × 100 / amount of free LPS in control samples.

3. Results

3.1. Antimicrobial activity

Compared to the natural AMP IN, four Trp-rich peptides (K_8W_3, K_7LW_3, $K_6L_2W_3$ and $K_5L_3W_3$) with +6 to +9 net positive charges displayed approximately 2-fold higher antimicrobial activities. The order of antimicrobial activity was $K_6L_2W_3$ > K_7LW_3, $K_5L_3W_3$ > K_8W_3 - $_5L_3W_3$ > K_8W_3 > $K_4L_4W_3$ > IN > $K_3L_5W_3$ $K_2L_6W_3$ (Table 2). Lys-containing peptides (K_8W_3, K_7LW_3 and $K_6L_2W_3$) showed approximately 2- to 4-fold higher antibacterial activities than did the counterpart Arg-containing peptides (R_8W_3, R_7LW_3 and $R_6L_2W_3$). $O_6L_2W_3$, $O_6X_2W_3$, $K_6L_2W_3$-D and $R_6L_2W_3$-D were 1.5-, 1.3-, 1.8-, and 1.5-fold less active than $K_6L_2W_3$, respectively. $R_6L_2W_3$-D was 1.5-fold more active than $R_6L_2W_3$.

3.2. Hemolytic activity

K_8W_3, K_7LW_3 and $K_6L_2W_3$ did not cause any hemolysis when present at concentrations up to 400 μM. In contrast, $K_5L_3W_3$, $K_4L_4W_3$, $K_3L_5W_3$ and $K_2L_6W_3$ induced significant hemolysis (5%) at 100 μM, 6.25 μM, 3.125 μM, and 1.56 μM, respectively (Table 3). The order of

Table 5
Tryptophan emission maxima of 3 μM solutions of peptides in the presence of 0.6 mM EYPE/EYPG (7:3, w/w) SUVs, and 0.6 mM EYPC/cholesterol (10:1, w/w) SUVs.

Peptide	Tris–HCl buffer (nm)	EYPE/EYPG (7:3, w/w) (nm)	EYPC/cholesterol (10:1, w/w) (nm)
K_8W_3	350.0	338.6 (11.4)	350.0 (0.0)
K_7LW_3	351.4	337.4 (14.0)	351.4 (0.0)
$K_6L_2W_3$	350.6	337.4 (13.2)	347.0 (3.6)
$K_5L_3W_3$	350.2	335.4 (14.8)	341.0 (9.2)
$K_4L_4W_3$	350.6	334.4 (16.2)	336.4 (14.2)
$K_3L_5W_3$	349.8	334.0 (15.8)	336.8 (13.0)
$K_2L_6W_3$	348.2	336.4 (11.8)	338.6 (9.6)
R_8W_3	351.0	340.6 (10.4)	346.6 (4.0)
R_7LW_3	350.0	341.8 (8.2)	346.6 (3.4)
$R_6L_2W_3$	350.0	338.0 (12.0)	340.8 (9.2)
$O_6L_2W_3$	350.6	339.4 (11.2)	346.4 (4.2)
$O_6X_2W_3$	352.0	338.8 (13.2)	344.8 (7.2)
$K_6L_2W_3$-D	350.2	335.4 (14.8)	344.4 (5.8)
$R_6L_2W_3$-D	350.2	338.4 (11.8)	340.0 (10.2)
Indolicidin (IN)	350.0	337.4 (12.6)	341.0 (9.0)

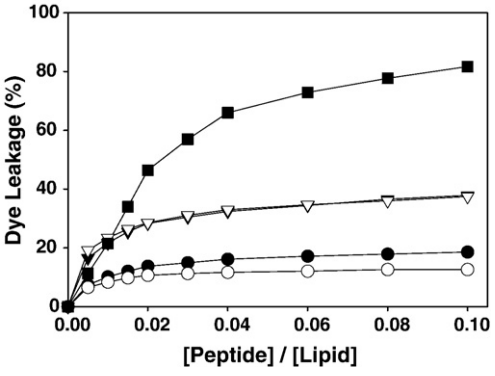

Fig. 3. Dose-dependent peptide-induced calcein release from negatively charged EYPE/EYPG (7:3, w/w) LUVs. The percentage of dye leakage caused by a peptide was calculated as follows: % Dye leakage = 100 × [($F - F_0$) / ($F_t - F_0$)], where F is the leaked fluorescence intensity achieved 5 min after addition of peptide, and F_0 and F_t are the intensities seen without the peptide and with Triton X-100 (full leakage; positive control), respectively. Peptides are indicated as follows: $K_6L_2W_3$ (●), $K_6L_2W_3$-D (○), $R_6L_2W_3$ (▼), $R_6L_2W_3$-D (▽), and Indolicidin (■).

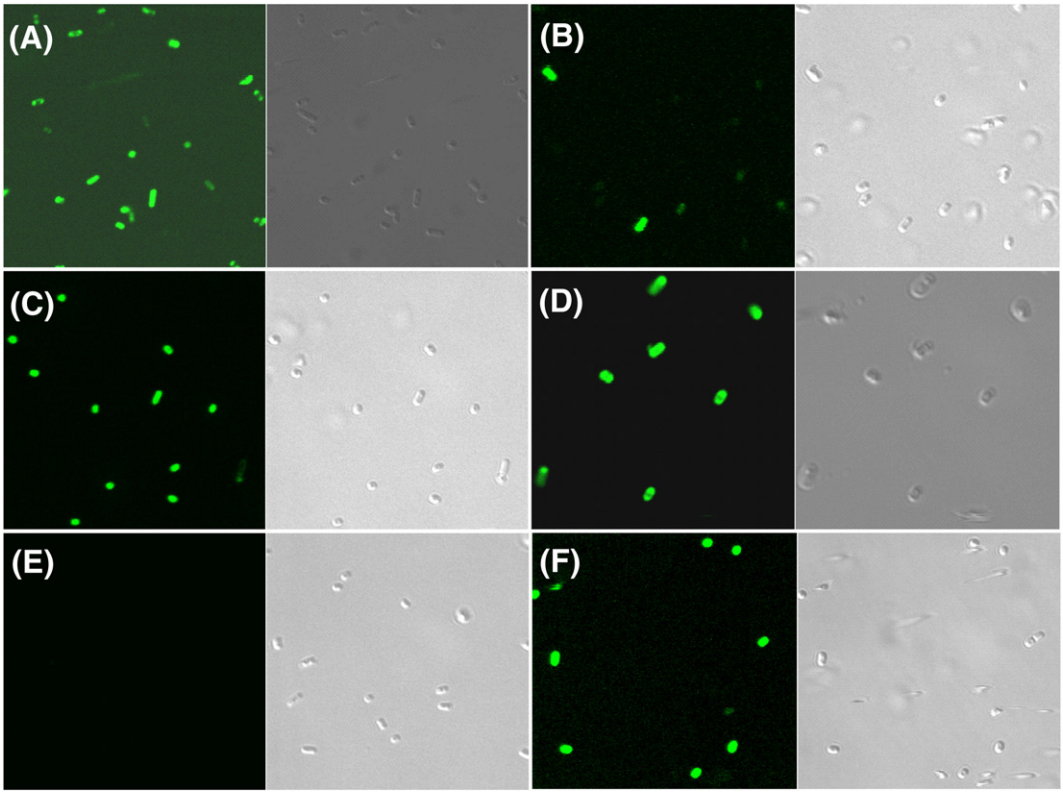

Fig. 4. Confocal laser-scanning microscopy of *E. coli* treated with FITC-labeled peptides. The cells were treated with 10 μg/ml of FITC-labeled $K_6L_2W_3$ (A), FITC-labeled $R_6L_2W_3$ (B), FITC-labeled $K_6L_2W_3$-D (C), FITC-labeled $R_6L_2W_3$-D (D), FITC-labeled IN (E), or FITC-labeled buforin-2 (F).

hemolytic activity for the peptides was $K_2L_6W_3$>$K_3L_5W_3$>$K_4L_4W_3$-$_2L_6W_3$>$K_3L_5W_3$>$K_4L_4W_3$>IN>$K_5L_3W_3$ K_8W_3, K_7LW_3, $K_6L_2W_3$ (Table 3). Interestingly, $K_6L_2W_3$ displayed no hemolytic activity up to 400 μM, but the counterpart Arg-containing peptide, $R_6L_2W_3$ displayed hemolytic activity at 400 μM. $O_6L_2W_3$ did not cause any hemolysis even at 400 μM, but $O_6X_2W_3$, $K_6L_2W_3$-D, and $R_6L_2W_3$-D induced significant hemolysis at 400 μM, 400 μM, and 200 μM, respectively. The retention time of peptides on a reverse-phase matrix was reported to be related to peptide hydrophobicity [40,41]. The relationships of the cationicity and hydrophobicity of our designed peptides between antimicrobial activity and hemolytic activity were investigated. Our results indicated that the cationicity of peptides is closely related to their antimicrobial activity and the hydrophobicity is in very good agreement with their hemolytic activity (Fig. 1).

3.3. Cell specificity/therapeutic index

To assess the cell specificity of the model peptides, we calculated the therapeutic index (TI), a widely accepted measurement of the cell specificity of an antimicrobial agent [42,43]. The therapeutic index of each peptide was calculated as the ratio of minimal hemolytic concentration (MHC) to GM. GM is the geometric mean of the MIC values seen when the peptides acted upon six bacterial strains (Table 3). The MHC is defined as the peptide concentration that produces 5% hemolysis. When no hemolytic activity was detectable at the highest concentration (400 μM) tested, an MHC of 800 μM was employed for therapeutic index calculation. A larger therapeutic index value corresponds to greater cell specificity. The therapeutic index of natural IN was 10.4, indicating relatively poor cell specificity. The therapeutic indices of K_8W_3, K_7LW_3 and $K_6L_2W_3$ were 320.0, 363.6, and 400.0 respectively. In particular, $K_6L_2W_3$ had the highest therapeutic index (~40-fold increase compared with IN). In contrast, $K_4L_4W_3$, $K_3L_5W_3$, and $K_2L_6W_3$ had very low therapeutic indices (between 0.1 and 1.9). Compared to Arg-containing peptides (R_8W_3, R_7LW_3 and $R_6L_2W_3$), the counterpart Lys-containing peptides (K_8W_3, K_7LW_3 and $K_6L_2W_3$) showed approximately a 2- to 4-fold higher cell specificity/therapeutic index than that of IN. In addition, the other peptides with unusual

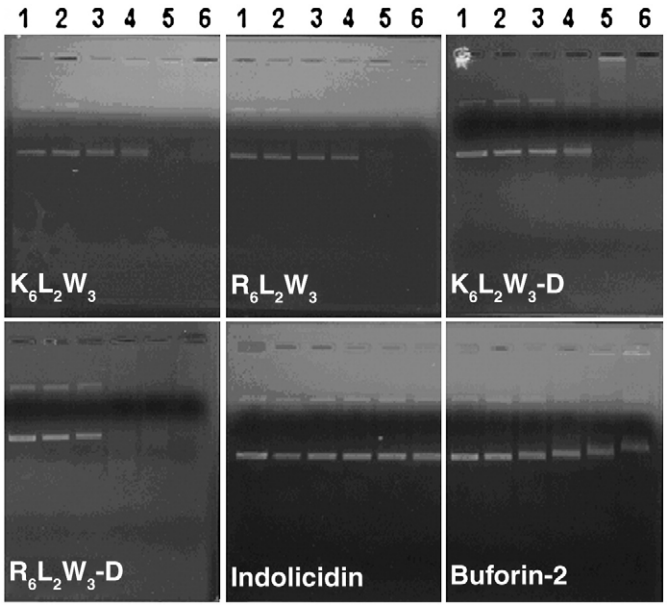

Fig. 5. Interaction of the peptides with plasmid DNA. Binding was assayed by measuring inhibition of plasmid DNA (100 ng; pBluscriptII SK^+) migration. DNA and peptides were co-incubated for 1 h at room temperature before electrophoresis on a 1.0% (w/v) agarose gel. Lane 1, plasmid DNA alone; lane 2, with 1 μM peptide; lane 3, with 2.5 μM peptide; lane 4, with 5 μM peptide; lane 5, with 10 μM peptide; and lane 6, with 20 μM peptide.

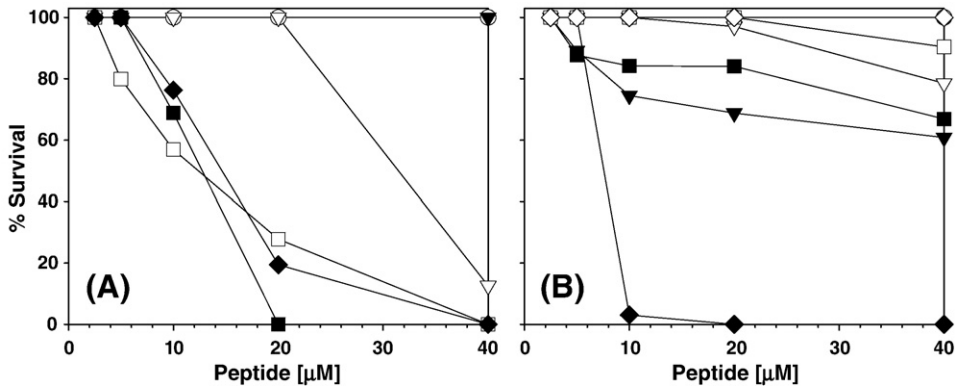

Fig. 6. Cytotoxicity of peptides against macrophage-derived RAW264.7 cells. Peptides are indicated as follows: (A) K_8W_3 (●), K_7LW_3 (○), $K_6L_2W_3$ (▼), $K_5L_3W_3$ (▽), $K_4L_4W_3$ (■), $K_3L_5W_3$ (□), $K_2L_6W_3$ (♦). (B) R_8W_3 (●), R_7LW_3 (○), $R_6L_2W_3$ (▼), $O_6L_2W_3$ (▽), $O_6X_2W_3$ (■), $K_6L_2W_3$-D (□), $R_6L_2W_3$-D (♦), and Indolicidin (◊).

amino acids ($O_6L_2W_3$, $O_6X_2W_3$, $K_6L_2W_3$-D and $R_6L_2W_3$-D) showed relatively high therapeutic indices between 111.1 and 266.6.

3.4. Antimicrobial activity against antibiotic-resistant clinical isolates

The antimicrobial activities of the model peptides against antibiotic-resistant clinical isolates were examined, to assess potential peptide usefulness as therapeutic agents (Table 4). Except for $K_2L_6W_3$, all model peptides displayed higher antimicrobial activities than did IN against two methicillin-resistant *Staphylococcus aureus* (MRSA) strains and two multidrug-resistant *Pseudomonas aeruginosa* (MDRPA) strains.

3.5. Resistance to proteolytic digestion

A major limitation of antimicrobial peptide is inactivation by proteases. Poor protease stability severely limits the clinical use of many therapeutic peptides [19,44]. We examined the susceptibility of peptides to trypsin. Trypsin specifically catalyzes the hydrolysis of C-terminal amide bonds of Lys and Arg, making the enzyme ideal for our

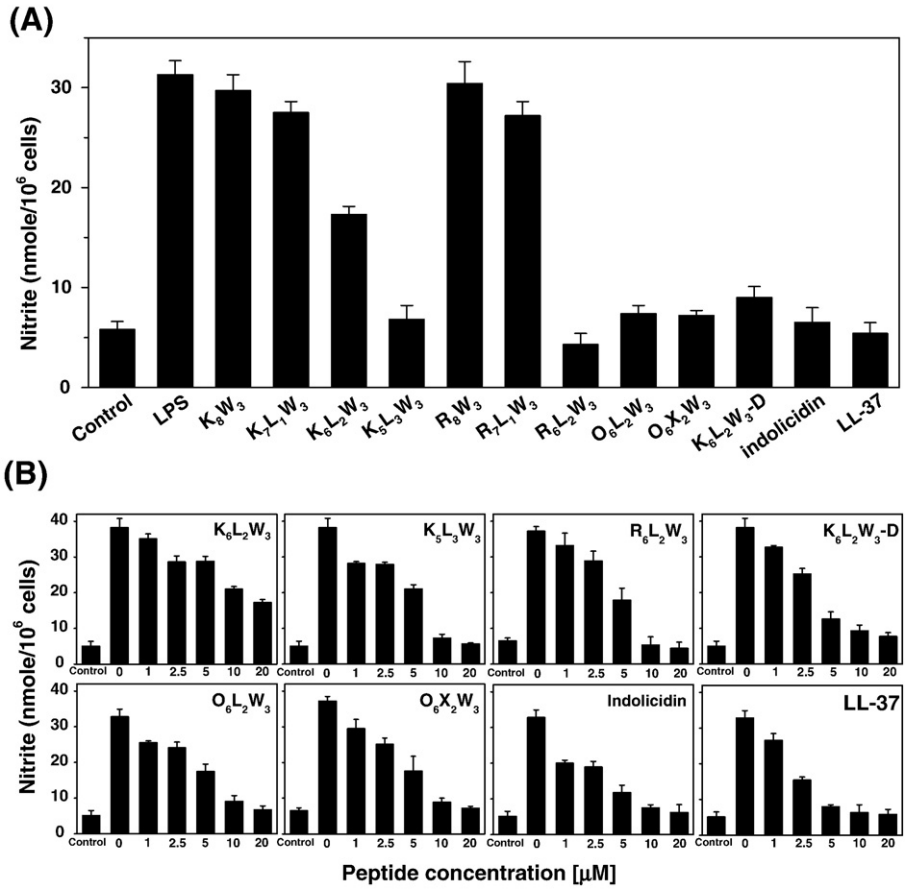

Fig. 7. Inhibitory effects of peptides on LPS-induced nitric oxide (NO) production in RAW264.7 cells. RAW264.7 cells (5×10^5 cells/ml) were treated with 20 ng/ml LPS in the absence or the fixed concentration (10 μM) (A) and the various concentrations (1, 2.5, 5, 10 and 20 μM) (B) of the peptides for 24 h. The cell culture media were then collected, and the amount of nitrite released within them was measured. The error bars represent standard deviations of the mean determined from three independent experiments.

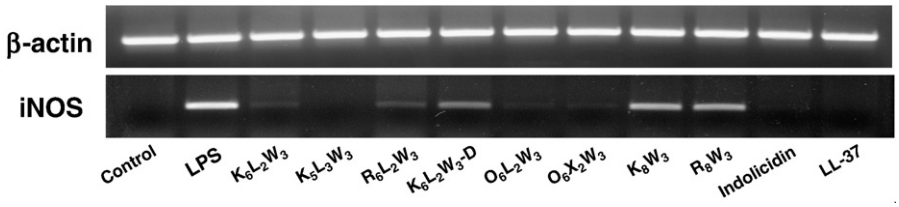

Fig. 8. Inhibitory effects of peptides on LPS-induced iNOS mRNAs expression in RAW264.7 cells. RAW264.7 cells (5×10^5 cells/well) were incubated with peptides (10 μM) in the presence of LPS (20 ng/ml) for 8 h. Total RNA was isolated and analyzed for expression of iNOS mRNA by RT-PCR. One of two representative experiments is shown.

work as our substrates contain multiple cleavage sites; the peptides possess several Lys or Arg residues. The assay was also used to examine whether peptides substituted with all D-amino acids, or with some Orn or/and Nle residues, might be stable to protease treatment. IN, $K_6L_2W_3$, $R_6L_2W_3$, $K_6L_2W_3$-D, $R_6L_2W_3$-D $O_6L_2W_3$, and $O_6X_2W_3$ were pretreated with trypsin and their residual antimicrobial activities assayed using the radial diffusion assay method and the broth microdilution assay method. As shown in Fig. 2, trypsin treatment of $K_6L_2W_3$, $R_6L_2W_3$, and IN with L-type amino acids abolished antimicrobial activities against both *E. coli* and *S. aureus*. However, the antimicrobial activities of $K_6L_2W_3$-D and $R_6L_2W_3$-D composed of D-type amino acids were stable even after trypsin treatment. In addition, trypsin treatment of $O_6L_2W_3$ and $O_6X_2W_3$ containing Orn or/and Nle, only partially decreased antimicrobial activity. These data reveal that substitution with unusual amino acids such as D-type amino acids, Orn or Nle, may allow sensitivity to enzymatic degradation to be controlled.

3.6. Tryptophan fluorescence blue shift in model membranes

When excited at 280 nm, Trp residues in the peptides, in aqueous buffer gave rise to an emission peak centered at 350 nm. When the peptides bound to phospholipids, the more hydrophobic environment and the decreased flexibility of the Trp residues caused a shift in this emission to lower wavelengths (the blue shift) (Table 5). In negatively charged EYPE/EYPG (7:3, w/w) SUVs, fluorescence emission maxima of all peptides exhibited a large blue shift, indicating that the peptides penetrated into the hydrocarbon region of the bilayer. In zwitterionic EYPC/cholesterol (10:1, w/w) SUVs, K_8W_3 and K_7LW_3 induced no blue shift in fluorescence emission maxima. In contrast, $K_6L_2W_3$, R_8W_3, R_7LW_3, $O_6L_2W_3$, and $K_6L_2W_3$-D caused moderate blue shift (3.4–5.8 nm), and the other peptides showed large blue shifts (7.2–14.2 nm). Compared to Lys-containing peptides (K_8W_3, K_7LW_3 and $K_6L_2W_3$), the counterpart Arg-containing peptides (R_8W_3, R_7LW_3 and $R_6L_2W_3$) showed larger blue shifts. Similar findings were observed in tritrpticin and analogs containing multiple Lys or Arg residues [15]. These results suggest that multiple Lys-containing peptides interact more weakly with zwitterionic phospholipids than do their multiple Arg-containing counterparts.

3.7. Calcein leakage from negatively charged model membranes

To examine whether the antimicrobial activities of $K_6L_2W_3$, $R_6L_2W_3$, $K_6L_2W_3$-D and $R_6L_2W_3$-D might depend on peptide ability to permeate bacterial membranes, we measured the influence of peptides on calcein leakage from negatively charged EYPE/EYPG (7:3 w/w) LUVs (a bacterial membrane-mimicking environment) (Fig. 3). IN was able to cause almost complete leakage of calcein at peptide/lipid molar ratio of 0.1, whereas $K_6L_2W_3$, $R_6L_2W_3$, $K_6L_2W_3$-D and $R_6L_2W_3$-D caused less than 40% dye leakage.

3.8. Confocal laser-scanning microscopy

To more precisely examine the localization of $K_6L_2W_3$, $R_6L_2W_3$, $K_6L_2W_3$-D and $R_6L_2W_3$-D, FITC-labeled peptides were incubated with *E. coli* and peptide distribution in the bacteria was investigated by confocal laser-scanning microscopy (Fig. 4). The antimicrobial activity of FITC-labeled peptides was identical to that of FITC-unlabeled peptides (data not shown). FITC-labeled $K_6L_2W_3$, $R_6L_2W_3$, $K_6L_2W_3$-D and $R_6L_2W_3$-D were found to penetrate the cell membrane and to accumulate inside *E. coli*, as observed for buforin-2, indicating that the cytoplasm is the major site of action of these peptides. In contrast, FITC-labeled IN did not enter the cell membrane.

3.9. DNA binding activity

To clarify the molecular mechanism of peptide action, we examined the DNA-binding properties of peptides (Fig. 5). DNA binding was examined by analyzing the electrophoretic mobility of DNA bands, at various ratios of peptide to DNA, on an agarose gel (1%, w/v), following earlier protocols used for testing of different antimicrobial peptides [45]. $K_6L_2W_3$, $R_6L_2W_3$, $K_6L_2W_3$-D, and $R_6L_2W_3$-D inhibited DNA migration at 5–10 μM. Buforin-2 significantly inhibited DNA migration at 20 μM, but IN did not inhibit DNA migration even at 20 μM.

3.10. Cytotoxicity

The cytotoxicities of peptides on RAW264.7 macrophage cells were evaluated by the standard MTT assay, which demonstrates active energization of cells and is conventionally used as a measure of cell viability. The result is shown in Fig. 6. Except for $K_4L_4W_3$, $K_3L_5W_3$, $K_2L_6W_3$, and $R_6L_2W_3$-D, no peptides exhibited significant cytotoxicity at 10 μM, as also observed for IN and LL-37. Furthermore, none of K_8W_3, K_7LW_3, $K_6L_2W_3$, R_8W_3, or R_7LW_3 exhibited any cytotoxicity even at 40 μM. Peptides showing no cytotoxicity at 10 μM were used in the experiments described below.

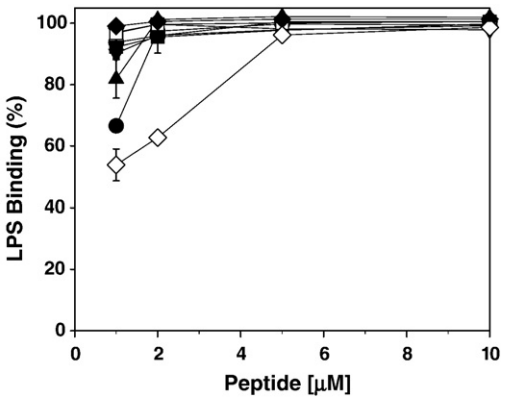

Fig. 9. LPS binding activity of the peptides. *E. coli*-derived LPS (*E. coli* O111:B4 LPS) (0.5 U/ml endotoxin) was incubated with various concentrations of each peptide for 30 min, and the amount of free LPS was determined using the *Limulus* amebocyte lysate assay. Peptides are indicated as follows: $K_6L_2W_3$ (●), $K_5L_3W_3$ (○), K6L2W3-D (▼), $R_6L_2W_3$ (▽), $O_6L_2W_3$ (■), $O_6X_2W_3$ (□), LL-37 (◆), Indolicidin (◊), and Polymyxin B (▲).

3.11. Inhibitory effect of peptides on nitric oxide (NO) production

Nitric oxide (NO) is one of the important inflammatory products and primarily involved in promoting inflammatory response. To assess the cells were treated with or without 20 ng/ml LPS at fixed or various concentration of peptides. Cell culture media were collected and stored at −70 °C. $K_5L_3W_3$, $R_6L_2W_3$, $O_6L_2W_3$, $O_6X_2W_3$, and $K_6L_2W_3$-D inhibited almost 100% of NO production at 10 μM, as observed for LL-37 and IN used as positive control peptides, but $K_6L_2W_3$ inhibited approximately 50% of NO production at 10 μM. In contrast, K_8W_3, K_7LW_3, R_8W_3, and R_7LW_3 had little effect on NO production at 10 μM (Fig. 7A). In addition, $K_5L_3W_3$, $R_6L_2W_3$, $O_6L_2W_3$, $O_6X_2W_3$, and $K_6L_2W_3$-D concentration-dependently inhibited NO production, with potencies similar to those shown by LL-37 and IN (Fig. 7B).

3.12. Inhibition of LPS-induced iNOS gene expression

LPS induces the expression of iNOS protein in macrophages, which correlates with NO production, so the effects of peptides on LPS-induced iNOS gene expression (LPS: 20 ng/ml) induced in LPS-stimulated RAW264.7 macrophage cells were examined over 6 h. $K_6L_2W_3$, $K_5L_3W_3$, $R_6L_2W_3$, $O_6L_2W_3$, $O_6X_2W_3$, and $K_6L_2W_3$-D at 10 μM completely suppressed iNOS gene expression. As expected, K_8W_3 and R_8W_3, which showed no inhibition of NO production, failed to exert any inhibitory effect on iNOS gene expression (Fig. 8). These data are in agreement with the NO production inhibition results of Fig. 7.

3.13. LPS binding activity

To determine whether the peptides might neutralize LPS at bactericidal concentrations, increasing concentrations of peptides were incubated with LPS and the resulting mixtures assessed using the LAL assay. $K_6L_2W_3$, $K_5L_3W_3$, $R_6L_2W_3$, $O_6L_2W_3$, $O_6X_2W_3$, and $K_6L_2W_3$-D displayed nearly complete LPS binding at 5 mM, as also observed for polymyxin B, IN and LL-37 (Fig. 9).

4. Discussion

In the present study, we successfully designed novel 11-meric Trp-rich model antimicrobial peptides with higher cell specificity than shown by the Trp-rich natural antimicrobial peptide, IN. We included only Trp, Lys/Arg, and Leu residues. K_8W_3, K_7LW_3 and $K_6L_2W_3$ displayed relatively high cell specificity/therapeutic index. In particular, $K_6L_2W_3$ exhibited the highest therapeutic index of 400.0 (approximately 40 times that of IN).

Although antimicrobial peptides show great structural diversity, all are cationic, because they have multiple Arg and/or Lys residues. This cationic property is very important for binding to negatively charged surfaces of bacteria lipid membranes. It has been reported that Arg→Lys substitution in a Trp-rich antimicrobial peptide, tritrpticin and an analog, increased cell specificity by enhancing antimicrobial activity and reducing hemolytic activity [15]. Also the effects of Lys and Arg residues of our Trp-rich model peptides on cell specificity were examined. As in previous report [15], Lys-containing peptides (K_8W_3, K_7LW_3, and $K_6L_2W_3$) showed approximately 2- to 4-fold higher cell specificities than did their counterpart Arg-containing peptides (R_8W_3, R_7LW_3, and $R_6L_2W_3$). These results suggest that multiple Lys residues are more important than multiple Arg residues in the design of antimicrobial peptides with improved cell specificity. In addition, the peptides were also very active against several clinical isolates, including MRSA and MDRPA, indicating that they may be promising lead compounds for the design of pharmaceuticals to overcome bacterial antibiotic resistance.

It has been known that the cell specificity of AMPs is mainly governed by the cationicity (net positive charge) and hydrophobicity of peptides, and there should be a proper balance between cationicity and hydrophobicity of peptides to retain potent antimicrobial peptides and avoid hemolytic activity [9–12]. Like other previous reports, the increase in cationicity of peptides promotes antimicrobial activity, whereas increases in hydrophobicity promote hemolytic activity. Among our designed Trp-rich peptides, $K_6L_2W_3$ had the most moderate cationicity and hydrophobicity to show potent antimicrobial activity and no hemolytic activity.

The suppression of antimicrobial peptide activity by proteolytic digestion has hampered efforts to develop safe and effective peptides for clinical use [19,44]. $K_6L_2W_3$ and $R_6L_2W_3$ composed of L-amino acids, were completely digested by trypsin. To increase proteolytic stability, Orn, Nle or D-type amino acids were substituted for L-amino acids of $K_6L_2W_3$ and $R_6L_2W_3$. The resulting analogs ($O_6L_2W_3$, $O_6X_2W_3$, $K_6L_2W_3$-D, and $R_6L_2W_3$-D) retained complete and partial antimicrobial activity even after trypsin treatment. Therefore, these peptides are candidate for clinical therapeutic use.

Most antimicrobial peptides have cationic and amphipathic properties and membrane disruption or pore/ion channel formation in cytoplasmic membranes of susceptible bacteria has been postulated as the main mode of action (*i.e.*, the membrane-targeting mechanism) [46,47]. Other mechanisms of action have been reported, including inhibition of cellular functions by binding to DNA, RNA, and proteins, and the inhibition of DNA, RNA, and/or protein synthesis (*i.e.*, the intracellular-targeting mechanism). For example, buforin-2, a cationic α-helical peptide isolated from the stomach of the Asian toad *Bufo bufo* gargarizans, exerts bactericidal activity, can penetrate cell membranes without lying susceptible bacteria, and binds more strongly to DNA and RNA than does magainin 2, [45,48]. PR-39 is bacteriostatic to Gram-negative bacteria and does not induce membrane lysis, nor does kill bacteria by a non-pore forming mechanism. Rather, PR-39 kills bacteria by a mechanism that stops protein and DNA synthesis after a lag period of about 8 min [49–51]. These results indicated that the antimicrobial actions of buforin-2 and PR-39 are in the class of intracellular target mechanisms.

A low ability to facilitate fluorescent marker escape from bacterial membrane-mimicking vesicles suggested that the principal bactericidal activities of several peptides ($K_6L_2W_3$, $R_6L_2W_3$, $K_6L_2W_3$-D, and $R_6L_2W_3$-D) might occur at sites inside bacteria. Therefore, to determine whether the peptides entered the bacterial cell membrane, visualization by confocal laser-scanning microscopy of FITC-labeled peptides was conducted. FITC-labeled $K_6L_2W_3$, $R_6L_2W_3$, $K_6L_2W_3$-D and $R_6L_2W_3$-D penetrated the cell membrane and accumulated in the cytoplasm of *E. coli*, as observed for buforin-2, whereas FITC-labeled IN did not enter the cell membrane. Furthermore, in gel retardation assays, we confirmed that $K_6L_2W_3$, $R_6L_2W_3$, $K_6L_2W_3$-D and $R_6L_2W_3$-D bound more strongly to DNA than did IN, as also seen with buforin-2. Taken together, these results suggest that a possible antimicrobial action mechanism of $K_6L_2W_3$, $R_6L_2W_3$, $K_6L_2W_3$-D, and $R_6L_2W_3$-D may be related to the inhibition of intracellular functions via interference with DNA/RNA synthesis.

Furthermore, to investigate whether our peptides might have anti-inflammatory activities when incubated with immune cells, as well as potent bactericidal activities, we examined the inhibition of the release of NO and iNOS mRNA expression by peptides in LPS-stimulated mouse macrophage RAW264.7 cells. Among our designed peptides, some, including $K_5L_3W_3$, $K_6L_2W_3$, $R_6L_2W_3$, $O_6L_2W_3$, $O_6X_2W_3$, and $K_6L_2W_3$-D suppressed LPS-induced inducible nitric oxide synthase (iNOS) mRNA expression and inhibited release of nitric oxide (NO) following LPS stimulation in RAW264.7 cells. In addition, these peptides had powerful LPS binding activities at bactericidal concentrations.

In conclusion, we successfully designed novel short Trp-rich model AMPs possessing high cell specificities and anti-inflammatory activities. These Trp-rich model AMPs have potential for future development as novel antimicrobial and anti-inflammatory peptides.

Acknowledgements

This study was supported by an ERC grant from the Ministry of Science and Technology, Korea and the Korea Science and Engineering Foundation through the Research Center for Proteineous Materials (R11-2000-083-00000-0) and by the research fund from Chosun University, 2008.

References

[1] H.G. Boman, Peptide antibiotics and their role in innate immunity, Annu. Rev. Immunol. 13 (1995) 61–92.
[2] R.I. Lehrer, T. Ganz, Antimicrobial peptides in mammalian and insect host defence, Curr. Opin. Immunol. 11 (1999) 23–27.
[3] R. Hancock, G. Diamond, The role of cationic antimicrobial peptides in innate host defences, Trends Microbiol. 8 (2000) 402–410.
[4] K.L. Brown, R.E. Hancock, Cationic host defense (antimicrobial) peptides, Curr. Opin. Immunol. 18 (2006) 24–30.
[5] M. Zasloff, Antimicrobial peptides of multicellular organisms, Nature 415 (2002) 389–395.
[6] R.E. Hancock, A. Patrzykat, Clinical development of cationic antimicrobial peptides: from natural to novel antibiotics, Curr. Drug Targets Infect. Disord. 2 (2002) 79–83.
[7] Z. Oren, Y. Shai, Mode of action of linear amphipathic α-helical antimicrobial peptides, Biopolymers 47 (1998) 451–463.
[8] A. Tossi, L. Sandri, A. Giangaspero, Amphipathic, α-helical antimicrobial peptides, Biopolymers 55 (2000) 4–30.
[9] R.F. Epand, R.I. Lehrer, W. Wang, R. Maget-Dana, D. Lelievre, R.M. Epand, Direct comparison of membrane interactions of model peptides composed of only Leu and Lys residues, Biopolymers 71 (2003) 2–16.
[10] L. Bven, S. Castano, J. Dufourcq, A. Wieslander, H. Wrblewski, The antibiotic activity of cationic linear amphipathic peptides: lessons from the action of leucine/lysine copolymers on bacteria of the class Mollicutes, Eur. J. Biochem. 270 (2003) 2207–2217.
[11] Y.M. Song, S.T. Yang, S.S. Lim, Y. Kim, K.S. Hahm, J.I. Kim, S.Y. Shin, Effects of L- or D-Pro incorporation into hydrophobic or hydrophilic helix face of amphipathic α-helical model peptide on structure and cell selectivity, Biochem. Biophys. Res. Commun. 314 (2004) 615–621.
[12] Y.M. Song, Y. Park, S.S. Lim, S.T. Yang, E.R. Woo, I.S. Park, J.S. Lee, J.I. Kim, K.S. Hahm, Y. Kim, S.Y. Shin, Cell selectivity and mechanism of action of antimicrobial model peptides containing peptoid residues, Biochemistry 44 (2005) 12094–12106.
[13] D.I. Chan, E.J. Prenner, H.J. Vogel, Tryptophan- and arginine-rich antimicrobial peptides: structures and mechanisms of action, Biochim. Biophys. Acta (2006) (1758) 1184–1202.
[14] D.J. Schibli, R.F. Epand, H.J. Vogel, R.M. Epand, Tryptophan-rich antimicrobial peptides: comparative properties and membrane interactions, Biochem. Cell Biol. 80 (2002) 667–677.
[15] S.T. Yang, S.Y. Shin, C.W. Lee, Y.C. Kim, K.S. Hahm, J.I. Kim, Selective cytotoxicity following Arg-to-Lys substitution in tritrpticin adopting a unique amphipathic turn structure, FEBS Lett. 540 (2003) 229–233.
[16] S.T. Yang, S.Y. Shin, Y.C. Kim, Y. Kim, K.S. Hahm, J.I. Kim, Conformation-dependent antibiotic activity of tritrpticin, a cathelicidin-derived antimicrobial peptide, Biochem. Biophys. Res. Commun. 296 (2002) 1044–1050.
[17] M.E. Selsted, M.J. Novotny, W.L. Morris, Y.Q. Tang, W. Smith, J.S. Cullor, Indolicidin, a novel bactericidal tridecapeptide amide from neutrophils, J. Biol. Chem. 267 (1992) 4292–4295.
[18] T.S. Ryge, X. Doisy, D. Ifrah, J.E. Olsen, P.R. Hansen, New indolicidin analogues with potent antibacterial activity, J. Pept. Res. 64 (2004) 171–185.
[19] A. Rozek, J.P. Powers, C.L. Friedrich, R.E. Hancock, Structure-based design of an indolicidin peptide analogue with increased protease stability, Biochemistry 42 (2003) 14130–14138.
[20] C.L. Friedrich, A. Rozek, A. Patrzykat, R.E. Hancock, Structure and mechanism of action of an indolicidin peptide derivative with improved activity against Gram-positive bacteria, J. Biol. Chem. 276 (2001) 24015–24022.
[21] C. Subbalakshmi, E. Bikshapathy, N. Sitaram, R. Nagaraj, Antibacterial and hemolytic activities of single tryptophan analogs of indolicidin, Biochem. Biophys. Res. Commun. 274 (2000) 714–716.
[22] C. Alexander, E.T. Rietschel, Bacterial lipopolysaccharides and innate immunity, J. Endotoxin Res. 7 (2001) 167–202.
[23] J. Cohen, The immunopathogenesis of sepsis, Nature 420 (2002) 885–918.
[24] Y. Rosenfeld, N. Papo, Y. Shai, Endotoxin (lipopolysaccharide) neutralization by innate immunity host-defense peptides. Peptide properties and plausible modes of action, J. Biol. Chem. 281 (2006) 1636–1643.
[25] S.M. Zughaier, W.M. Shafer, D.S. Stephens, Antimicrobial peptides and endotoxin inhibit cytokine and nitric oxide release but amplify respiratory burst response in human and murine macrophages, Cell Microbiol. 7 (2005) 1251–1262.
[26] Y. Rosenfeld, Y. Shai, Lipopolysaccharide (endotoxin)-host defense antibacterial peptides interactions: role in bacterial resistance and prevention of sepsis, Biochim. Biophys. Acta 1758 (2006) 1513–1522.
[27] M. Yoshioka, N. Fukuishi, Y. Kubo, H. Yamanobe, K. Ohsaki, Y. Kawasoe, M. Murata, A. Ishizumi, Y. Nishii, N. Matsui, M. Akagi, Human cathelicidin CAP18/LL-37 changes mast cell function toward innate immunity, Biol. Pharm. Bull. 31 (2008) 212–216.
[28] R.E. Hancock, Cationic peptides: effectors in innate immunity and novel antimicrobials, Lancet Infect. Dis. 1 (2001) 156–164.
[29] D.M. Bowdish, D.J. Davidson, M.G. Scott, R.E. Hancock, Immunomodulatory activity of small host defense peptides, Antimicrob. Agents Chemother. 49 (2005) 1727–1732.
[30] R.E. Hancock, M.G. Scott, The role of antimicrobial peptides in animal defenses, Proc. Natl. Acad. Sci. U. S. A. 97 (2000) 8856–8861.
[31] I. Nagaoka, S. Hirota, F. Niyonsaba, M. Hirata, Y. Adachi, H. Tamura, D. Heumann, Cathelicidin family of antibacterial peptides CAP18 and CAP11 inhibit the expression of TNF-alpha by blocking the binding of LPS to CD14 (+) cells, J. Immunol. 167 (2001) 3329–3338.
[32] D. Mao, B.A. Wallace, Differential light scattering and absorption flattening optical effects are minimal in the circular dichroism spectra of small unilamellar vesicles, Biochemistry 23 (1984) 2667–2673.
[33] Y. Shai, D. Bach, A. Yanovsky, Channel formation properties of synthetic pardaxin and analogues, J. Biol. Chem. 265 (1990) 20202–20209.
[34] C.R. Barlett, Phosphorus assay in column chromatography, J. Biol. Chem. 234 (1959) 466–468.
[35] D.A. Scudiero, R.H. Shoemaker, K.D. Paull, A. Monks, S. Tierney, T.H. Nofziger, M.J. Currens, D. Seniff, M.R. Boyd, Evaluation of a soluble tetrazolium/formazan assay for cell growth and drug sensitivity in culture using human and other tumor cell lines, Cancer Res. 48 (1988) 4827–4833.
[36] L.C. Green, D.A. Wagner, J. Glogowski, P.L. Skipper, J.S. Wishnok, S.R. Tannenbaum, Analysis of nitrate, nitrite, and [^{15}N]nitrate in biological fluids, Anal. Biochemistry 126 (1982) 131–138.
[37] Y.J. Jeon, S.B. Han, K.S. Ahn, H.M. Kim, Activation of NF-kappaB/Rel in angelan-stimulated macrophages, Immunopharmacology 43 (1999) 1–9.
[38] B.F. Tack, M.V. Sawai, W.R. Kearney, A.D. Robertson, M.A. Sherman, W. Wang, T. Hong, L.M. Boo, H. Wu, A.J. Waring, SMAP-29 has two LPS-binding sites and a central hinge, Eur. J. Biochem. 269 (2002) 1181–1189.
[39] Y. Xiao, H. Dai, Y.R. Bommineni, J.L. Soulages, Y.X. Gong, O. Prakash, G. Zhang, Structure-activity relationships of fowlicidin-1, a cathelicidin antimicrobial peptide in chicken, FEBS J. 273 (2006) 2581–2593.
[40] T. Kiyota, S. Lee, G. Sugihara, Design and synthesis of amphiphilic α-helical model peptides with systematically varied hydrophobic–hydrophilic balance and their interaction with lipid- and bio-membranes, Biochemistry 35 (1996) 13196–13204.
[41] S. Kim, S.S. Kim, B.J. Lee, Correlation between the activities of α-helical antimicrobial peptides and hydrophobicities represented as RP-HPLC retention times, Peptides 26 (2005) 2050–2056.
[42] Y. Chen, C.T. Mant, S.W. Farmer, R.E. Hancock, M.L. Vasil, R.S. Hodges, Rational design of α-helical antimicrobial peptides with enhanced activities and specificity/therapeutic index, J. Biol. Chem. 280 (2005) 12316–12329.
[43] W.L. Zhu, Y.M. Song, Y. Park, K.H. Park, S.T. Yang, J.I. Kim, I.S. Park, K.S. Hahm, S.Y. Shin, Substitution of the leucine zipper sequence in melittin with peptoid residues affects self-association, cell selectivity, and mode of action, Biochim. Biophys. Acta 1768 (2007) 1506–1517.
[44] K. Hamamoto, Y. Kida, Y. Zhang, T. Shimizu, K. Kuwano, Antimicrobial activity and stability to proteolysis of small linear cationic peptides with D-amino acid substitutions, Microbiol. Immunol. 46 (2002) 741–749.
[45] C.B. Park, H.S. Kim, S.C. Kim, Mechanism of action of the antimicrobial peptide buforin II: buforin II kills microorganisms by penetrating the cell membrane and inhibiting cellular functions, Biochem. Biophys. Res. Commun. 244 (1998) 253–257.
[46] Y. Shai, Mode of action of membrane active antimicrobial peptides, Biopolymers 66 (2002) 236–248.
[47] M. Dathe, T. Wieprecht, Structural features of helical antimicrobial peptides: their potential to modulate activity on model membranes and biological cells, Biochim. Biophys. Acta 1462 (1999) 71–87.
[48] C.B. Park, K.S. Yi, K. Matsuzaki, M.S. Kim, S.C. Kim, Structure-activity analysis of buforin II, a histone H2A-derived antimicrobial peptide: the proline hinge is responsible for the cell-penetrating ability of buforin II, Proc. Natl. Acad. Sci. U. S. A. 97 (2000) 8245–8250.
[49] L. Tomasinsig, B. Skerlavaj, N. Papo, B. Giabbai, Y. Shai, M. Zanetti, Mechanistic and functional studies of the interaction of a proline-rich antimicrobial peptide with mammalian cells, J. Biol. Chem. 281 (2006) 383–391.
[50] M. Cudic, L. Otvos Jr., Intracellular targets of antibacterial peptides, Curr. Drug Targets 3 (2002) 101–106.
[51] H.G. Boman, B. Agerberth, A. Boman, Mechanisms of action on *Escherichia coli* of cecropin P1 and PR-39, two antibacterial peptides from pig intestine, Infect. Immun. 61 (1993) 2978–2984.